

December 2007

Comparison between patterns generated by microcontact printing and dip-pen nanolithography on

Heeyeon P. Wampler

Purdue University - Main Campus, park7@purdue.edu

Dmitry Zemlyanov

Birck Nanotechnology Center, Purdue University, dimazemlyanov@purdue.edu

Albena Ivanisevic

Birck Nanotechnology Center, Purdue University, albena@purdue.edu

Follow this and additional works at: <http://docs.lib.purdue.edu/nanopub>

Wampler, Heeyeon P.; Zemlyanov, Dmitry; and Ivanisevic, Albena, "Comparison between patterns generated by microcontact printing and dip-pen nanolithography on" (2007). *Birck and NCN Publications*. Paper 303.
<http://docs.lib.purdue.edu/nanopub/303>

This document has been made available through Purdue e-Pubs, a service of the Purdue University Libraries. Please contact epubs@purdue.edu for additional information.

Comparison between Patterns Generated by Microcontact Printing and Dip-Pen Nanolithography on InP Surfaces

Heeyeon P. Wampler, Dmitry Y. Zemlyanov, and Albena Ivanisevic

J. Phys. Chem. C, **2007**, 111 (49), 17989-17992 • DOI: 10.1021/jp077554+

Downloaded from <http://pubs.acs.org> on January 9, 2009

More About This Article

Additional resources and features associated with this article are available within the HTML version:

- Supporting Information
- Links to the 1 articles that cite this article, as of the time of this article download
- Access to high resolution figures
- Links to articles and content related to this article
- Copyright permission to reproduce figures and/or text from this article

[View the Full Text HTML](#)



Comparison between Patterns Generated by Microcontact Printing and Dip-Pen Nanolithography on InP Surfaces

Heeyeon P. Wampler,[†] Dmitry Y. Zemlyanov,[‡] and Albena Ivanisevic^{*,†,‡}

Department of Chemistry, Birck Nanotechnology Center, and Weldon School of Biomedical Engineering, Purdue University, West Lafayette, Indiana 47907

Received: September 19, 2007; In Final Form: October 29, 2007

InP surfaces were patterned by microcontact printing and dip-pen nanolithography (DPN). The chemical nature and coverage of the functionalized surfaces were evaluated by X-ray photoelectron spectroscopy. The presence of all adsorbates on the surface was verified. The XPS data confirmed the covalent attachment of the adsorbates when microcontact printing was used, but no evidence for covalent bonding was observed when InP was patterned by DPN.

Introduction

In recent decades, a number of unconventional lithographic approaches have been established as useful fabrication tools for variety of micro- and nanostructures.¹ For example, microcontact printing has been used to pattern small organic molecules as well as biomolecules.^{2,3} Scanning probe lithography-based approaches have also been utilized to deliver different adsorbates and have produced structures on the order of a few nanometers.^{4–7} In many cases, the capabilities of these techniques have been primarily explored on metal surfaces such as gold. Furthermore, the attachment of the desired molecular patterns has been primarily accomplished through a covalent bond with a thiol functionality.

We recently began to characterize the chemical and morphological differences between patterns generated by microcontact printing and dip-pen nanolithography (DPN)^{8–13} on III–V semiconductor surfaces such as GaAs.¹⁴ Such evaluation can be done using surface-sensitive techniques like X-ray photoelectron spectroscopy (XPS).¹⁵ The information obtained can be very useful in determining which lithographic method is suitable for the functionalization of devices composed of III–V materials. Such semiconductor surfaces have been used to construct field-effect transistors and light-emitting diodes and can, in principle, participate in novel sensing strategies.

We recently compared the ability of alkanethiols and short synthetic peptides to form covalent bonds to InP surfaces.¹⁶ In addition, we quantified the coverage and tilt angles of these adsorbates on the same surface. In this paper, we report the quantitative characterization of InP surfaces functionalized by microcontact printing and DPN. We characterize the type of bonding obtained with the same adsorbates when the two different lithographic methods are used. In addition, we note differences in surface coverage obtained when lithography is used instead of adsorption from solution.

Three different adsorbates were evaluated: 1-octadecanethiol (ODT), 6-mercapto-1-hexanol (MHL), and a short peptide sequence, CGISYGRKKRRQRRR. We have previously used these adsorbates on InP, GaP, and GaAs surfaces to form self-assembled monolayers using adsorption from solution. Prior to any patterning and after cleaning and oxide removal, the InP surface was fairly hydrophilic (contact angle = $28 \pm 0.5^\circ$) and smooth (roughness = 0.28 ± 0.06 nm). Representative microcontact printing patterns are shown in Figure 1. Contact angles measured over areas completely covered with large features of ODT, MHL, and peptide were 91.0 ± 2.35 , 35.2 ± 3.27 , and $29.2 \pm 1.30^\circ$, respectively. We note that the contact angle differences after the modification with the peptide and MHL may be due to the fact that hydrophobic parts of the molecules are exposed on the surface as a result of a less-ordered assembly. The roughness values calculated from the evaluation of areas completely covered with the microcontact printed patterns of ODT, MHL, and peptide were 0.23 ± 0.01 , 0.21 ± 0.01 , and 2.80 ± 0.46 nm, respectively. From the AFM height and lateral force microscopy (LFM) images of alkanethiol patterns, one can see evidence for the formation of monolayers in the desired areas. The peptide features can be clearly identified in the height images, and one can see large differences in the packing within the stamped stripes when high-resolution AFM is done.

DPN was utilized to pattern the same adsorbates on InP, Figure 2. The speed used to pattern ODT and MHL was $9.85 \mu\text{m/s}$ at 34–37% relative humidity and a temperature of 23°C . The writing speed used to generate the peptide lines was also $9.85 \mu\text{m/s}$, but the relative humidity was 75–80%, and the temperature was 23°C . The structures shown in this figure were rinsed with solvent after the patterning process, allowed to dry for 24 h, and then imaged with clean tips. The LFM images show the expected differences in contrast between hydrophobic and hydrophilic inks. In addition, features written with MHL and the peptide are more clearly seen in the height images compared to the ones generated with ODT. The roughness values measured for the patterns generated by DPN and the three inks were 0.43 ± 0.15 , 0.41 ± 0.07 , and 0.76 ± 0.53 nm for

* To whom correspondence should be addressed. Tel.: 765-496-3676. Fax: 765-496-1459. E-mail: albena@purdue.edu.

[†] Department of Chemistry.

[‡] Birck Nanotechnology Center.

[‡] Weldon School of Biomedical Engineering.

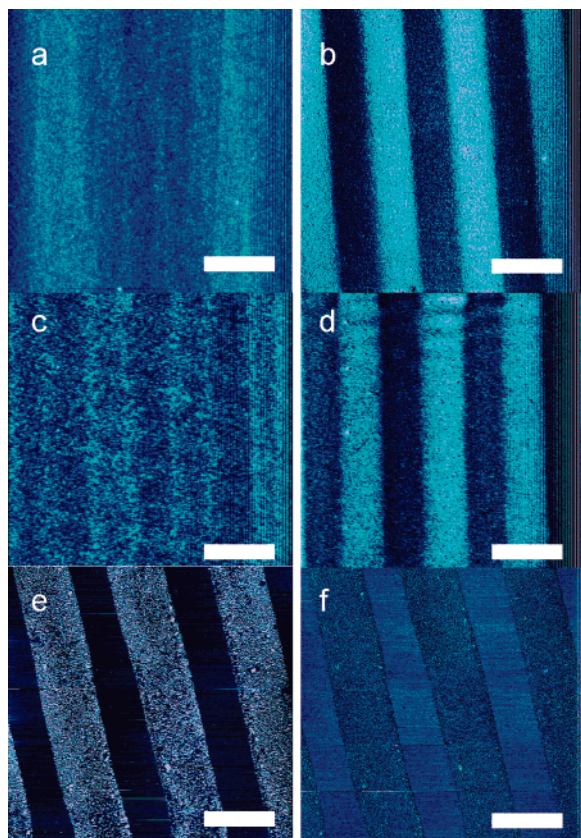


Figure 1. InP surfaces patterned with ODT (a and b), MHL (c and d), and peptide (e and f) using microcontact printing. The images on the left are height and on the right LFM. All images were collected using clean tips. The scan sizes were $20\ \mu\text{m} \times 20\ \mu\text{m}$, and the scan speed was 4.07 Hz. The scale bar is $5\ \mu\text{m}$.

ODT, MHL, and peptide, respectively. These values are slightly higher than ones measured on patterns generated by microcontact printing, and we believe that this is due to differences in surface coverages between the two types of lithographic features. As a result of the AFM characterization, we gathered evidence that well-defined features can be placed in desired patterns by either lithographic method on InP. However, this type of characterization does not give quantitative information in terms of the chemical bonding to the surface and coverage of molecules per surface area. We utilized a surface-sensitive analytical technique, XPS, in order to quantitatively compare the two lithographic procedures.

XPS is a technique widely used to access the chemical composition of surfaces.¹⁷ We developed a micron-size alignment marker to collect spectra from a specific region on the surface where the lithographic patterns were located. Initially, XPS was used to qualitatively compare the type of chemical bonding between the surface and each adsorbate when a specific lithographic procedure was done. High-resolution spectra of the following regions were collected to understand the surface composition: In 3d, P 2p, C 1s, N 1s, and S 2p. The high-resolution spectra of the S 2p region obtained after InP was modified by microcontact printing with ODT and MHL clearly showed the presence of S and supports the notion that adsorption occurred. The data collected with these adsorbates was consistent with previous reports.¹⁶ The surface microcontact printed with a peptide ink demonstrated a weak S signal, whereas no S could be detected after patterning by DPN. On substrates patterned by DPN with the two alkanethiol inks, we observed peaks at $\sim 168\ \text{eV}$, which indicated that the adsorbates were present on the surface but were oxidized.¹⁸ It is noteworthy that XPS

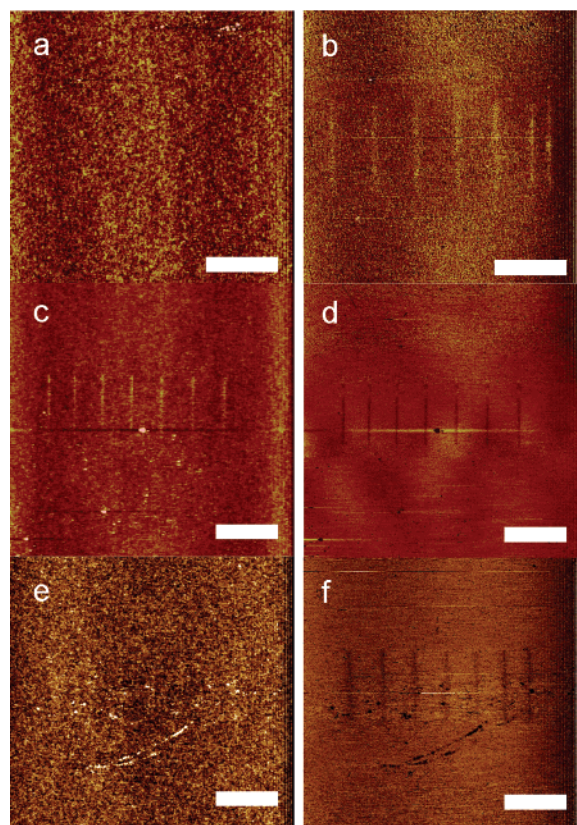


Figure 2. InP surfaces patterned with ODT (a and b), MHL (c and d), and peptide (e and f) using DPN. The images on the left are height and on the right LFM. All images were collected using clean tips. The scan sizes were $20\ \mu\text{m} \times 20\ \mu\text{m}$, and the scan speed was 3.59 Hz. The scale bar is $5\ \mu\text{m}$.

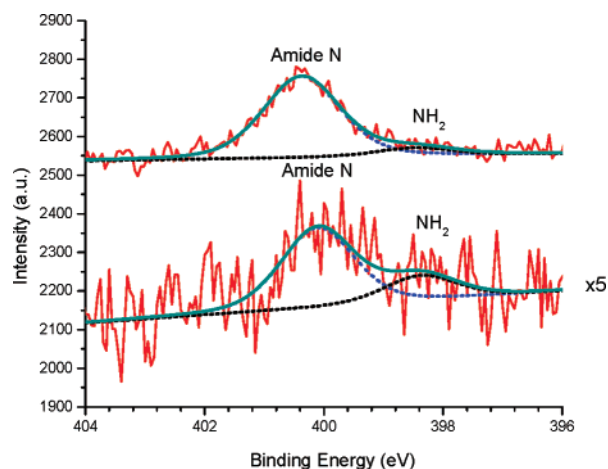


Figure 3. High-resolution XPS spectra of the N 1s region; (1) InP surface patterned by microcontact printing and (2) InP surface patterned by DPN. In both cases the peptide was used as an ink. The intensity difference between the two sets of data is due to a different adsorption area.

detected all characteristic elements, indicating that all adsorbates were present on the surface regardless of which lithographic protocol was used. Such evidence was collected by examining the C 1s and N 1s spectra. Figure 3 shows the typical N 1s spectra along with the curve-fitting results, which revealed peaks corresponding to hydrocarbon species when a peptide ink was used. The DPN patterns that we generated for the XPS analysis are $100\ \mu\text{m} \times 100\ \mu\text{m}$. However, the beam size during the XPS analysis is 10 times bigger than the generated structure. This is the reason for

TABLE 1: Summary of Coverage Values (Number of Molecules Per nm²) Extracted from the XPS Data; for Surfaces Modified with a Peptide Ink, the Exact Amount of Carbon Was Calculated from Curve Fitting

samples	C (In 3d _{5/2} /P 2p)	N (In 3d _{5/2} /P 2p)
μ -cp-ODT	1.68/2.61	
DPN-ODT	1.46/2.35	
μ -cp-MHL	4.20/6.69	
DPN-MHL	4.52/7.53	
μ -cp-peptides	0.19/0.30	0.07/0.11
DPN-peptides	0.08/0.13	0.02/0.03
solution peptides ^a		0.91/1.12

^a These data are based on ref 16, where adsorption from solution was used to modify the InP with peptides.

the difference in the signal-to-noise level. We anticipate that coverage on the surface will vary based on the writing speed. In addition, the presence of -C-N-, amide C, and N species was verified in the C 1s spectra of samples modified by microcontact printing and DPN.

The XPS data were also used to determine the surface coverage of the patterned InP surfaces. The coverage was determined using the nonattenuating adlayer approximation proposed by Fadley.¹⁹ It is important to note that the kinetics of ink transport from the tip to the surface play a key role in the final composition of the patterns on the surface. We believe that differences in such kinetics can influence the surface coverage by different inks on the surface and plan to investigate this in more detail during future studies. The film coverage using Fadley's formalism was reproducibly determined using a nonattenuating adlayer approximation. The curve-fitting procedure produced a $\sim 10\%$ error. The calculations were based on the ratio between the photoelectron peaks from the substrate and the adsorbate and have been previously described.²⁰ NIST SRD-82²¹ was utilized to calculate the electron attenuation length, which was used instead of the inelastic mean free path (IMFP). We used the intensities of the In 3d_{5/2} and P 2p peaks for the substrate and the C 1s and N 1s peaks for the adsorbed layer. Since the S 2p peak was very weak, in order to minimize the error, we did not incorporate the S 2p data in the calculations. The coverage values extracted from the XPS data are summarized in Table 1. In the case of peptide ink, the exact amount of carbon was calculated using curve fitting, and the residual hydrocarbon contribution was subtracted. The coverages calculated based on the presence of just C species on the surface were not significantly different between the two lithographic protocols. A more significant difference between the two lithographic methods can be seen for peptides. The other remarkable feature is that coverages calculated based on P 2p data are always higher than those obtained based on In 3d_{5/2} data. This points to the enrichment of the surface region with indium. One can make a direct comparison between the peptide coverage data collected on surfaces functionalized from solution and the ones modified by a lithographic protocol. Such coverages were calculated using the N atoms on the surface. The coverage of peptides on the surface is lower when lithography is used to anchor the molecules on the surface. The coverage of alkanethiols on InP (ODT = 0.457 molecules/nm²; MHL = 0.246 molecules/nm²)¹⁶ and on Au (4.16 molecules/nm²)²² has been previously reported based on calculations involving the presence of S atoms on the surface and tritium labeling studies. Since the S 2p peak was extremely weak on substrates modified by DPN, a direct comparison with such literature data is not possible.

In conclusion, we collected data that enabled the comparison between microcontact printing and DPN on InP surfaces. Our evaluation showed that all adsorbates were present on the surface regardless of which lithographic protocol was used. The coverage of biomolecules on InP was generally lower when lithography was used to deliver the adsorbates to the surface compared to data obtained from functionalizing the same substrates using adsorption from solution. We anticipate incorporating the finding of this work into future studies that utilize microfabricated devices that contain InP regions.

Experimental Section

Reagents and Materials: Fe-doped ($4.5 \times 10^8 \text{ cm}^{-3}$) *n*-InP (100) wafers were obtained from Crystacomm (Mountain View, CA). 1-Octadecanethiol (ODT), 98%, and 6-mercapto-1-hexanol, 97%, were purchased from Aldrich. All other solvents were purchased from Mallinckrodt Chemicals. SYLGARD 184 silicon elastomer base and curing agent were purchased from Dow Corning Corporation (Midland, MI). The peptide, CGISYGRKKRRRQRRR, was synthesized by AnaSpec (San Jose, CA), purified by HPLC, and analyzed by MALDI-TOF.

Surface Preparation: Small pieces of InP ($0.5 \times 0.5 \text{ cm}^2$) were consecutively cleaned by ultrasonication with three solvents, acetone, methanol, and isopropanol. Subsequently, each surface was immersed in concentrated HF solution (49%) for 10 min to remove oxides on the surface. The InP substrates were then rinsed with water and isopropanol.

Microcontact Printing (μ -CP): All solutions were prepared with a 1 mM concentration. The PDMS stamps were prepared according to the manufacturer's specifications. To carry out the stamping, PDMS pads were rinsed with ethanol and dried with nitrogen. The PDMS stamps were gently wiped with a Q-tip soaked in the solutions. The stamps were then contacted to the surfaces for ~ 30 s. After stamping, the surfaces were rinsed with solvent.

Dip-Pen Nanolithography (DPN): Solutions with concentrations of 5 (alkanethiols in ethanol) and 10 mM (peptide in PBS buffer) were used as inks. The surfaces were evaluated using a Multi-Mode Nanoscope IIIa from Digital Instruments. The AFM was housed in a home-built chamber to maintain specific temperature and humidity conditions. The AFM probes used in the lithography experiments were purchased from Veeco, Model No. MSC-T-AUHW, and had a spring constant of 0.05 N/m. The tips were coated with ODT, MHL, and TAT peptides by allowing the tips to soak in a desired solution for 10 min. Patterning of each ink was done using a standard DPN protocol under the conditions stated in the text. The roughness of the patterns was evaluated using the rms values. The rms is defined as the root-mean square average of the height deviation taken from the mean data plane

$$R_q = \sqrt{\left(\sum Z_i^2\right)/n}$$

The data we collected showed that there are no meaningful differences after the modifications.

X-ray Photoelectron Spectroscopy (XPS): For the XPS analysis, all features generated by either DPN or μ -CP covered a total area of $100 \times 100 \mu\text{m}^2$ to accommodate the spatial resolution of the technique. XPS data were obtained by a Kratos Ultra DLD spectrometer using monochromatic Al K α radiation. The survey and high-resolution spectra were collected at fixed

analyzer pass energies of 160 and 20 eV, respectively. The spectra were collected at a 0° angle with respect to the surface normal. All data analysis was done with the commercially available software package CasaXPS. The binding energy (BE) values were referenced to C 1s at 284.80 eV.

Acknowledgment. This work was supported by NSF under CHE-0614132.

Supporting Information Available: Additional data regarding the characterization of the patterns by XPS and AFM. This material is available free of charge via the Internet at <http://pubs.acs.org>.

References and Notes

- (1) Xia, Y. N.; Rogers, J. A.; Paul, K. E.; Whitesides, G. M. *Chem. Rev.* **1999**, *99*, 1823.
- (2) Geissler, M.; Bernard, A.; Bietsch, A.; Schmid, H.; Michel, B.; Delamar, E. *J. Am. Chem. Soc.* **2000**, *122*, 6303.
- (3) Lahiri, J.; Ostuni, E.; Whitesides, G. M. *Langmuir* **1999**, *15*, 2055.
- (4) Piner, R. D.; Zhu, J.; Xu, F.; Hong, S. H.; Mirkin, C. A. *Science* **1999**, *283*, 661.
- (5) Salaita, K.; Lee, S. W.; Wang, X.; Huang, L.; Dellinger, T. M.; Liu, C.; Mirkin, C. A. *Small* **2005**, *1*, 940.
- (6) Zhang, H.; Amro, N. A.; Disawal, S.; Elghanian, R.; Shile, R.; Fragala, J. *Small* **2007**, *3*, 81.
- (7) Agarwal, G.; Sowards, L. A.; Naik, R. R.; Stone, M. O. *J. Am. Chem. Soc.* **2003**, *125*, 580.
- (8) Lenhart, S.; Sun, P.; Wang, Y.; Fuchs, H.; Mirkin, C. A. *Small* **2007**, *3*, 71.
- (9) Nafday, O. A.; Weeks, B. L. *Langmuir* **2006**, *22*, 10912.
- (10) Lee, K. B.; Lim, J. H.; Mirkin, C. A. *J. Am. Chem. Soc.* **2003**, *125*, 5588.
- (11) Jang, J. W.; Maspoth, D.; Fujigaya, T.; Mirkin, C. A. *Small* **2007**, *3*, 600.
- (12) Hampton, J. R.; Dameron, A. A.; Weiss, P. S. *J. Am. Chem. Soc.* **2006**, *128*, 1648.
- (13) Weeks, B. L.; DeYoreo, J. J. *J. Phys. Chem. B* **2006**, *110*, 10231.
- (14) Cho, Y.; Ivanisevic, A. *Langmuir* **2006**, *22*, 8670.
- (15) Petrovykh, D. Y.; Kimura-Suda, H.; Tarlov, M. J.; Whitman, L. J. *Langmuir* **2004**, *20*, 429.
- (16) Park, H. H.; Ivanisevic, A. *J. Phys. Chem. C* **2007**, *111*, 3710.
- (17) Petrovykh, D. Y.; Kimura-Suda, H.; Whitman, L. J.; Tarlov, M. J. *J. Am. Chem. Soc.* **2003**, *125*, 5219.
- (18) McGuinness, C. L.; Shaporenko, A.; Mars, C. K.; Uppili, S.; Zharnikov, M.; Allara, D. L. *J. Am. Chem. Soc.* **2006**, *128*, 5231.
- (19) Fadley, C. S. Basic Concepts of X-ray Photoelectron Spectroscopy. In *Electron Spectroscopy: Theory, Techniques, and Application*; Brundle, C. R., Baker, A. D., Eds.; Academic Press: London; Vol. 2, 1978.
- (20) Jedlicka, S. S.; Rickus, J. L.; Zemlyanov, D. Y. *J. Phys. Chem. B* **2007**, *111*, 11850.
- (21) *NIST SRD-82*, 1.1 ed., National Institute Standard Technology: Gaithersburg, MD, 2001.
- (22) Dubois, L. H.; Nuzzo, R. G. *Annu. Rev. Phys. Chem.* **1992**, *437–463*, 437.